Heliyon 10 (2024) e35066

Contents lists available at ScienceDirect

Heliyon

journal homepage: www.cell.com/heliyon

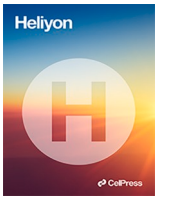

Research article

Spectral and chemical characterization of amber from Xixia, Henan Province, China via FTIR, three-dimensional fluorescence spectra and Py (HMDS)-GC-MS

Yan Li [a,b,**,1], Yilei Feng [a,1], Jingfen Du [a,c], Yamei Wang [a,d,*], Guanghai Shi [e], Youzhi Liang [f]

[a] Gemological Institute, China University of Geoscience, Wuhan, 430074, China
[b] Hubei Engineering Research Center of Jewelry, Wuhan, 430074, China
[c] Cultural Heritage and Art Design Institute, Zhengzhou University of Technology, Zhengzhou, 450000, China
[d] Guangzhou CUG Gems and Jewelry Testing Co. Ltd, Guangzhou, China
[e] School of Gemology, China University of Geosciences, Beijing, 100083, China
[f] Central Academy of Fine Arts, Chaoyang District, Beijing, 100102, China

ARTICLE INFO

Keywords:
Fossil resins
Xixia amber
Infrared spectroscopy
Fluorescence
Py-GC-MS

ABSTRACT

Xixia amber from Henan Province in China has undergone a thorough examination utilizing microscopic observation, infrared spectroscopy, and three-dimensional (3D) fluorescence spectroscopy. This systematic analysis has revealed that there are primarily two varieties of Xixia amber: a light-colored type and a dark-colored type. These can be differentiated based on their coloration, infrared spectra, and distinctive fluorescence attributes. Notably, the infrared spectral profile of Xixia amber features a prominent peak at 1023 cm^{-1}, accompanied by less pronounced peaks at 1088 and 974 cm^{-1}. These spectral characteristics set it apart from amber originating from the Baltic regions, Myanmar, and Fushun. Further distinction is achieved through 3D fluorescence spectra, where Xixia amber exhibits similarities to Burmese and Fushun ambers. Chemical classification via pyrolysis gas chromatography-mass spectrometry (Py-GC-MS) identifies Xixia amber as belonging to Class Ib, characterized by its ordered structure and the absence of succinic acid. This comprehensive study delineates the coloration, infrared spectral properties, photoluminescent behavior, and chemical compositions of Xixia amber, clearly differentiating it from ambers sourced from other geographical locations.

1. Introduction

Amber, an enchanting organic gemstone, forms through extensive geological processes spanning millions to billions of years. This unique material primarily originates from the fossilized resin of ancient plants, primarily from the Late Cretaceous to the Miocene epoch within the Cenozoic era [1]. Its historical usage dates back to the Stone Age, approximately 10,000 years ago. Amber has held significant roles in human history, not only as a medicinal agent but also as a material for crafting artifacts and jewelry, illustrating its

* Corresponding author. Gemological Institute, China University of Geoscience, Wuhan, 430074, China.
** Corresponding author. Gemological Institute, China University of Geoscience, Wuhan, 430074, China.
E-mail addresses: yanli@cug.edu.cn (Y. Li), wangym@cug.edu.cn (Y. Wang).
[1] co-first authors.

https://doi.org/10.1016/j.heliyon.2024.e35066
Received 11 March 2024; Received in revised form 22 July 2024; Accepted 22 July 2024
Available online 31 July 2024

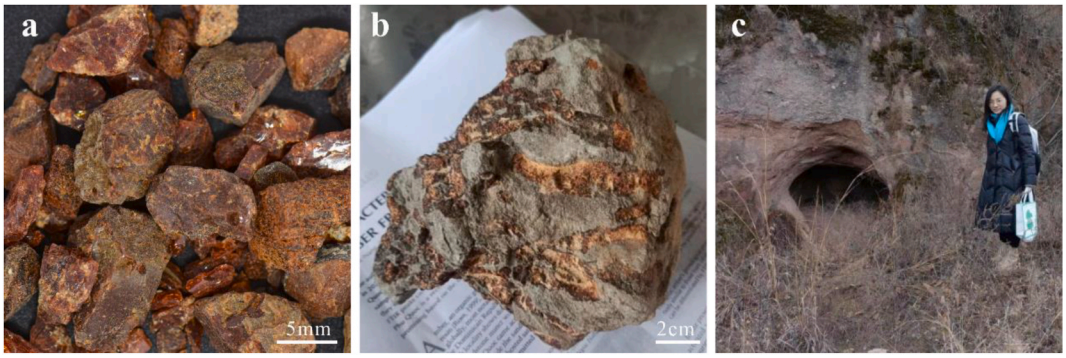

Fig. 1. (a) Amber fragments collected the from local villagers; (b) Specimen provided by villagers for photos; (c) The site where a large nest of amber was dug up more than 40 years ago in Sigou Village, Chongyang Township.

profound impact on historical and cultural development and communication globally. Amber mines, presented in over 100 countries excluding Antarctica, show a highly uneven distribution of reserves: about 90 % are located in the Baltic Sea coastal regions, with other significant sources in the Americas, particularly the Dominican Republic and Mexico, and in Asia, notably in Burma and Japan [2].

In China, prominent amber sources include Fushun in Liaoning, Zhangpu in Fujian, and other areas such as Xixia in Henan, Enshi in Hubei, Lijiang in Yunnan, Hunchun in Jilin, and Nanning in Guangxi [3]. The amber mining history in Xixia is particularly notable, with records dating back to ancient times. Since the 1950s, mining in this region has been primarily carried out by individuals and, to a lesser extent, by collective efforts. Many local villagers have privately owned rough amber materials (Fig. 1a and b). And there are accounts of significant amber findings, including a clutch of amber weighing several hundred kilograms discovered over 40 years ago [4] (Fig. 1c).

The use of amber in China boasts a rich history that extends approximately 4000 years into the past. The earliest known artifact is a heart-shaped amber pendant excavated from the No. 1 sacrificial pit at the Sanxingdui site in Guanghan, Sichuan [5]. Amber holds significant value in Chinese culture, not only as a gemstone but also for its traditional medicinal uses. It was firstly documented as 'Yupei' in the Classic of the Mountains and Seas (770-220 BCE). The term 'hupo', meaning amber, appeared later in the Xinyu written by Lujia during the Western Han Dynasty. Since then, amber artifacts have been unearthed from almost every historical dynasty, affirming its continuous importance in Chinese culture. Its medicinal applications, rooted in ancient pharmacology texts like *Lei Gong's Treatise on Preparation and Boiling of Materia Medica* from the North and South Dynasties, were further elaborated upon in Li Shizhen's *Compendium of Materia Medica* from the Ming Dynasty. These texts highlight amber's efficacy in calming the mind, promoting blood circulation, and serving as an amulet for protection.

In recent years, advancements in the study of amber's molecular structure and compositional characteristics have been markedly enhanced through the application of spectroscopic characterization technologies, including Fourier Transform Infrared (FTIR) spectroscopy, Raman spectroscopy, nuclear magnetic resonance (NMR), and three-dimensional (3D) fluorescence spectra. These techniques offer rapid, straightforward, and non-destructive or minimally invasive analytical methods, eliminating the need for complex sample preparation procedures. Notably, FTIR spectroscopy has played a pivotal role in comparing ambers from diverse origins and geological epochs [6], effectively unveiling information about organic functional groups in both pristine and oxidized amber. Significant increases in C=O groups (within the spectral range of 1760 to 1665 cm-1) have been observed in aged Baltic amber [7] and Burmese amber [8], contributing to the understanding of the transformations amber undergoes over time.

Moreover, the evolution of fluorescence analysis techniques has highlighted the unique fluorescent properties of amber when exposed to long-wave ultraviolet radiation. Both conventional two-dimensional fluorescence spectra and advanced three-dimensional fluorescence spectra have been integrated into amber research methodologies. Comparative studies investigating the effects of artificial aging (using 340 nm ultraviolet light, light exposure, and a temperature of 90 °C) on the fluorescence of fossil resins from various locations have demonstrated that as artificial aging progresses, there is a decrease in the intensity of fluorescence excitation and emission spectra, accompanied by a redshift in the peak wavelength [9]. Three-dimensional fluorescence and phosphorescence spectra have been employed to analyze the photoluminescent characteristics of different varieties of Burmese amber. It has been revealed that an increase in carbonyl groups (C=O) correlates with the redshift of the fluorescence peak in Burmese blood amber [10]. The diversity in the types of amber can be attributed to the disparities in the original resin secretions [11].

Despite the presence of China's largest known amber deposit in Xixia, research utilizing spectral analysis on Xixia amber is remarkably scarce. This particular type of amber is distinguished by its rich color range and considerable differences in fluorescence intensity. To delve into the distinctions among differently colored Xixia samples and to draw comparisons with amber from other significant global locations, this study has selected eight raw amber specimens in yellow-brown hues from Henan Province's Xixia, along with three yellow-toned amber samples from diverse origins, including the Baltic region, Burma, and Fushun in China. The objective is to perform infrared and fluorescence spectroscopy analyses to elucidate and contrast the spectral properties of these specimens.

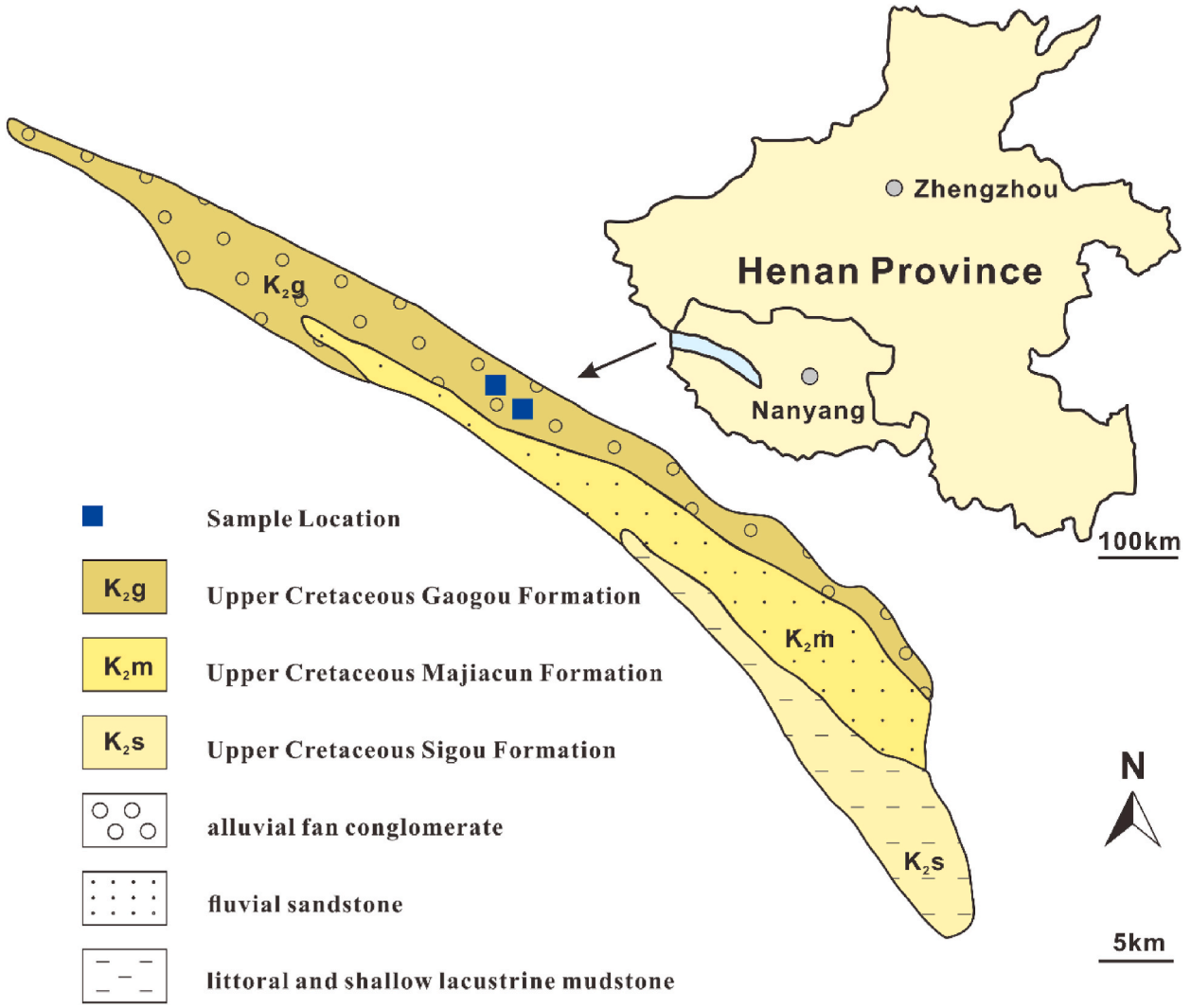

Fig. 2. Xixia Basin, modified according to Zhang et al. (2002) [12] & Cao et al. (2010) [16].

2. Geological context of the Xixia Basin

The Xixia Basin, located within Henan Province, is characterized as a Mesozoic sedimentary basin oriented predominantly along a NW-SE axis. As part of a series of geological basins that have extended in a NW-SE direction since the Late Cretaceous, this basin is situated on the southern side of the central orogenic belt of the East Qinling Mountains. Its boundaries are demarcated by faults to the north and south. Its foundation is primarily composed of Aurignacian or Hercynian granite, which is overlaid by a substantial thickness—exceeding 3000 m—of gray-green lacustrine and alluvial-phase red conglomerates and sandstones. The strata generally trend NW and gently dip SW, with typical angles ranging between 10° and 20° [12].

The basin exclusively features Upper Cretaceous formations, which are exceptionally well-preserved and can be sequentially stratified divided into the Gaogou, Majiacun, and Sigou Formations, in ascending order [4] (Fig. 2). The amber-bearing strata are predominantly located within the lower portion of the Gaogou Formation, dating back approximately 70 million years [13]. As there is currently no indication that the amber in this region has experienced secondary sedimentation, the age of the amber is presumed to correspond with the stratigraphic age. This particular formation is distinguished by its extensive interbedded conglomerates, coarse sandstones, and purplish-red mudstones, with a notable thickness of 596 m. It overlies discordantly on the metamorphic rocks of various ages constituting the basin's basement [12] and is renowned for its inclusion of exceptionally preserved dinosaur eggs [14,15].

The amber was predominantly discovered within rock formations distinguished by conglomeratic layers interspersed with purplish-red or grayish, grayish-white fine to medium sandstone. These conglomerates are primarily composed of quartzite, diorite, and various metamorphic rocks. The distribution pattern of the amber exhibits an enrichment trend that slopes downward and eastward, with a corresponding decrease in grain size. This trend correlates with the basin's evolutionary history, characterized by uplift in the west and subsidence in the east [12].

Fig. 3. Amber samples used in this study. Eight amber samples from Xixia, Henan Province: two yellow samples, Y-1 and Y-2, one light brown sample, LB, three orange samples, O-1, O-2 and O-3, and two brown samples, B-1 and B-2 (A is the interior, and B is the crust). Three amber samples of other origins: E−1 from the Baltic Sea, E−2 from Burma, and E−3 from Fushun, China.

In investigating the botanical origins of the amber found in the Xixia Basin, Zhou et al. (2005) posited a Late Triassic source [4]. The Late Cretaceous climate of the Xixia Basin was marked by its heat and aridity, with sparse vegetation, which would have been unlikely to produce copious amounts of resin. In contrast, the more favorable conditions of a warmer climate and abundant vegetation during the Late Triassic period present a more probable setting for resin production. This resin, initially expelled during the petrification stage of coal formation, would have then been subject to increased concentration due to recurring environmental shifts, including tectonic uplifts and dry periods. Unlike typical air-exposed resins that often contain fossilized insects, Xixia amber, transported and deposited in sandstones and conglomerates, lacks such inclusions. Molecular analysis suggests that the Xixia amber likely originated from the Araucariaceae family of conifers, a group that is primarily found in the Southern Hemisphere today but was widespread in the Northern Hemisphere during the Mesozoic era [17]. This evidence supports the earlier hypotheses concerning the origins of the amber.

3. Materials and methods

3.1. Samples

3.1.1. Xixia samples

A collection of nine distinct amber specimens, alongside two specimens still encased within their host rocks and two bags of amber fragments, were gathered from two locations within the Xixia region: Caogang Township and Chayu Village. Of this assemblage, nine specimens—eight separate pieces and one within its host rock—originated from Caogang Village and Chayu Village. Thin sections of the specimens embedded in their host rocks were prepared for examination under a microscope. These samples are illustrated in Fig. 3a.

3.1.2. Reference samples

To facilitate comparative analysis, additional amber samples sourced from the Baltic Sea, Burma, and Fushun in Liaoning, China (Fig. 3a E−1, E−2, and E−3) were incorporated into the study. These reference samples were acquired from the gemstone testing center at China University of Geosciences in Guangzhou, each with a confirmed provenance tracing back to their origin mines.

3.2. Experimental methods and test conditions

Tests were completed at Gemmological Institute, China University of Geosciences, Wuhan.

Photography and Physical Testing. Samples were illuminated with a D65 light source (Macbeth, 6500 K, 20 W) and photographed under neutral gray conditions. The specific gravity of the samples was measured using a hydrostatic pressure meter, and their refractive index was determined using a standard gemological refractometer.

Table 1
Basic Gemological properties of Xixia amber samples.

Sample no.	SG	Color	RI	UV fluorescence
Y-1	1.043	Yellow	1.56	Strong, blue
Y-2	1.048	Yellow	1.54	Strong, blue
O-1	1.000	Orange	1.57	Weak, blue
O-2	1.133	Orange	1.59	Weak, blue
O-3	1.111	Orange	1.58	Weak, blue
LB	1.043	Light Brown	1.55	Strong, blue
B-1	1.040	Dark Brown	1.53	Middle, blue
B-2	1.083	Dark Brown	1.58	Middle, blue

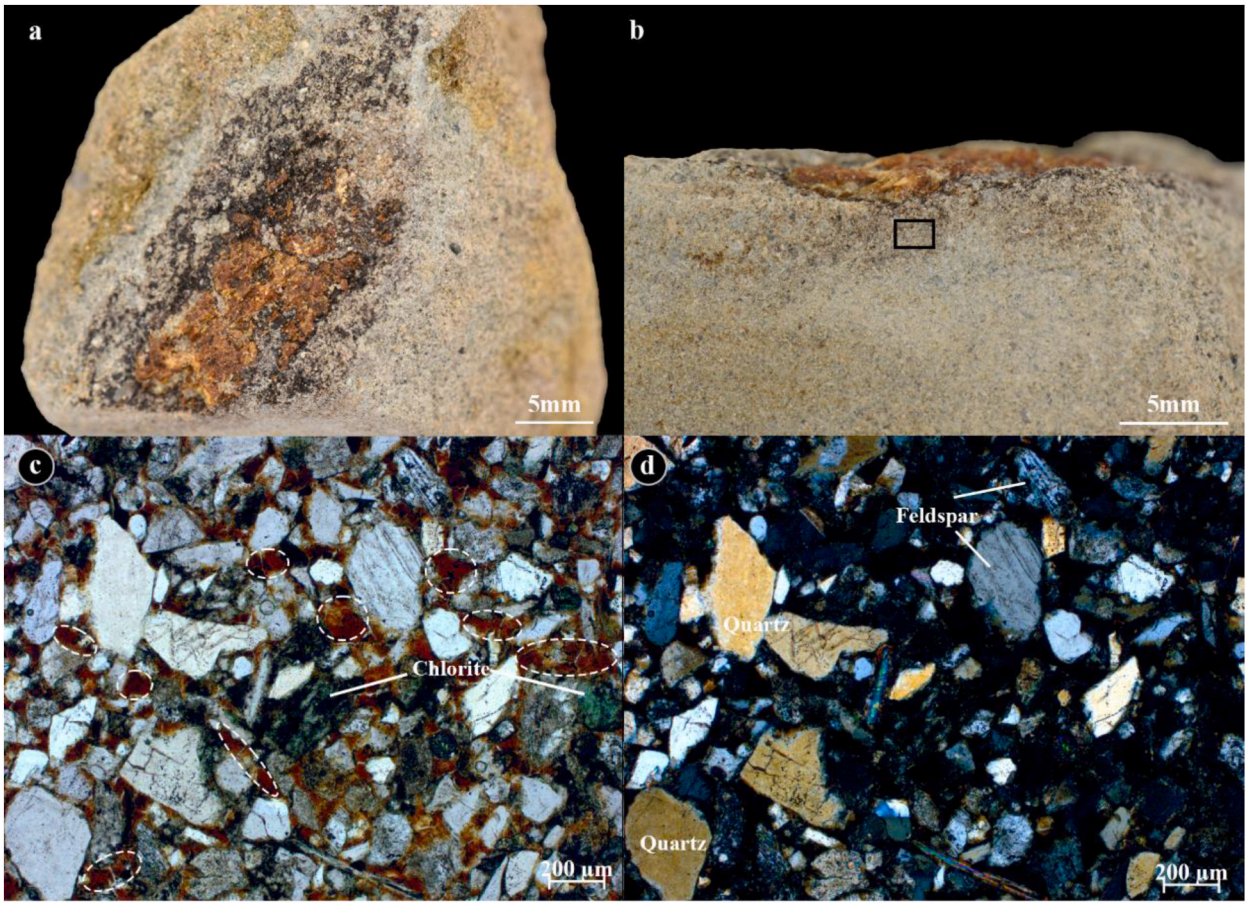

Fig. 4. (a) Amber-bearing rock. The square in the side view picture of the rock (b) indicates the viewing areas of Fig. 4c and d. Thin-section photomicrographs were taken in transmitted light using parallel polarisers (c) and crossed polarisers (d).

Microscopic Observation. Thin slices of amber-bearing sandstone, approximately 3 μm thick, were examined under a Zeiss petrographic microscope in transmission mode with orthogonal polarization (90°). Internal features were further observed using a Leica M205A/DFC 550 micro camera at magnifications ranging from 12.5 to 256.

Fourier Transform Infrared Spectroscopy. The Fourier transform infrared (FTIR) absorption spectra were recorded using a Bruker Vertex 80 FTIR spectrometer in the mid-infrared range (4000 cm^{-1} to 400 cm^{-1}). To capture detailed absorption peaks in the fingerprint region (1500 cm^{-1} to 400 cm^{-1}), the KBr pellet transmission method was used. Samples were mixed with potassium bromide (KBr) at a mass ratio of 1:100 to 1:200, ground, and pressed into pellets. Background scans were conducted 32 times, and sample scans were performed 64 times, with a resolution of 2 cm^{-1}.

Fluorescence Spectroscopy. Fluorescence checks on all samples were performed with a standard 4 W long-wave UV lamp (365 nm). Solid amber three-dimensional fluorescence spectroscopy was conducted using a JASCO FP-8500. Solid samples were examined using the EFA-833 solid sample accessory in a 45° geometry arrangement for the light source-sample-detector. The surface method, as proposed by Briks (1967), was employed to characterize the fluorescence emission spectra of solid amber at various excitation

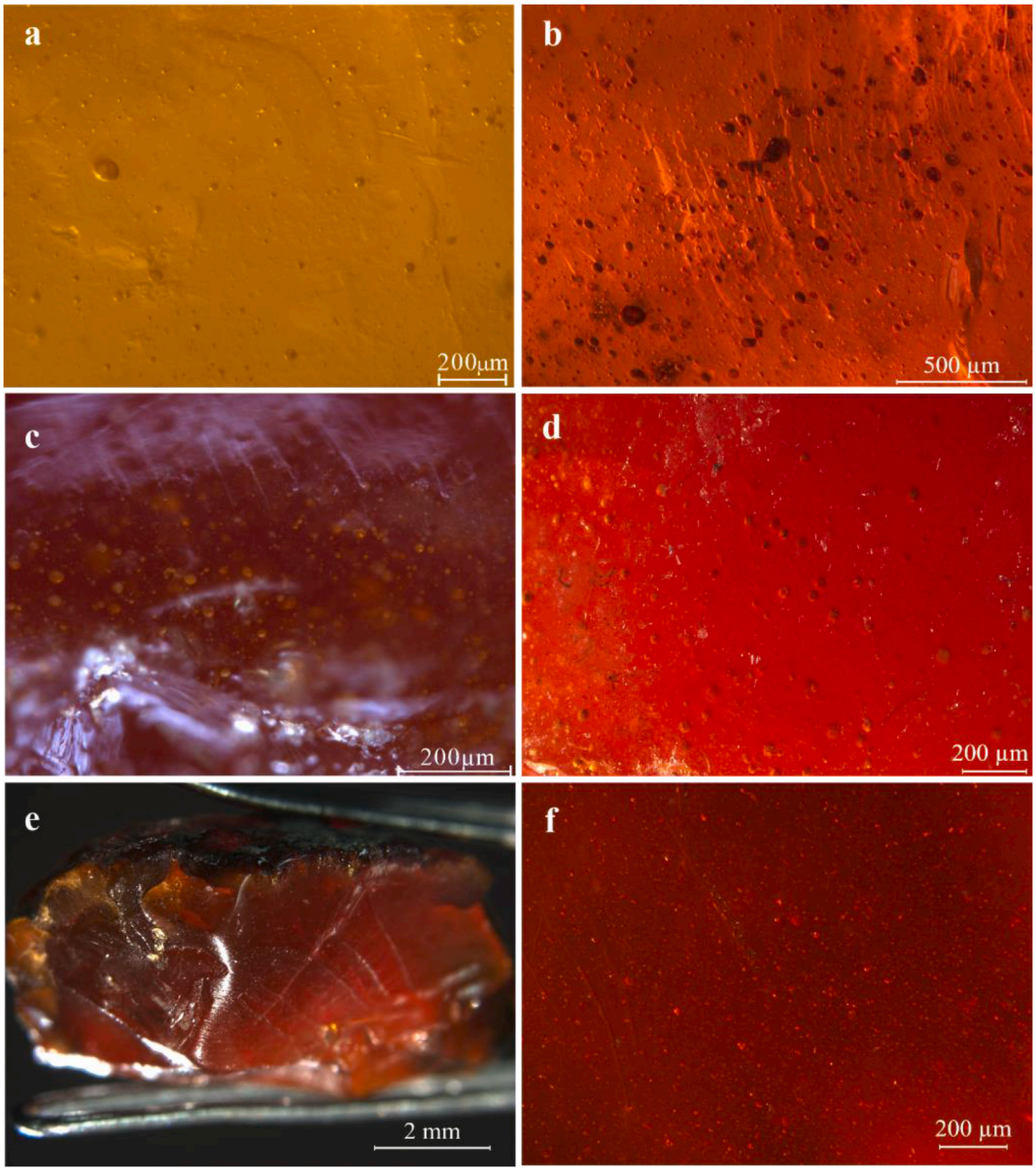

Fig. 5. Internal features of Xixia amber samples: (a) tiny bubbles in the yellow sample Y-1; (b) dark inclusions and small bubbles in the light-brown sample LB; (c, d) large number of bubbles in the orange samples O-2 and O-3; (e) profiles of brown sample B-2; (f) tiny bubbles in the brown sample B-1.

wavelengths. Given the different times of sample acquisition, slight adjustments were made to the testing parameters: excitation wavelength range of 220 nm–600 nm with a bandwidth of 5 nm and data interval of 2 nm; emission wavelength range of 240 nm–750 nm with a bandwidth of 5 nm and data interval of 1 nm; detector response time of 0.5 s; HT voltage set at 350V; photomultiplier tube (PMT) voltage in the detector set to low; and scanning speed of 1000 nm/min. Data were plotted based on excitation wavelength, emission wavelength, and fluorescence intensity. Additionally, two-dimensional fluorescence spectra (emission wavelength vs. intensity) for the optimal excitation wavelength of 365 nm were also generated.

Pyrolysis-Gas Chromatography-Mass Spectrometry. Pyrolysis experiments were conducted using a pyrolyzer (CDS Pyroprobe 5000 series), and GC/MS analysis was carried out using a gas chromatograph/mass spectrometer (6890A GC/5975C MSD, Agilent, U.S.A.). HMDS (hexamethyldisilazane, AR, 98 %), a silylation derivatizing reagent, was obtained from Macklin and used without further modification. To investigate and compare the resinous fossil characteristics of Burmese and Xixia amber, two sets of samples were tested. The first set consisted of a mixture of Burmese and Xixia samples, while the second set comprised solely of Xixia samples. Py/GC/MS analysis proceeded as follows: For each analysis, approximately 1 mg of the samples was placed in a sample cup, and 5 μL of the derivatizing agent was added. Subsequently, the samples were introduced into the heated quartz tube and subjected to pyrolysis at a

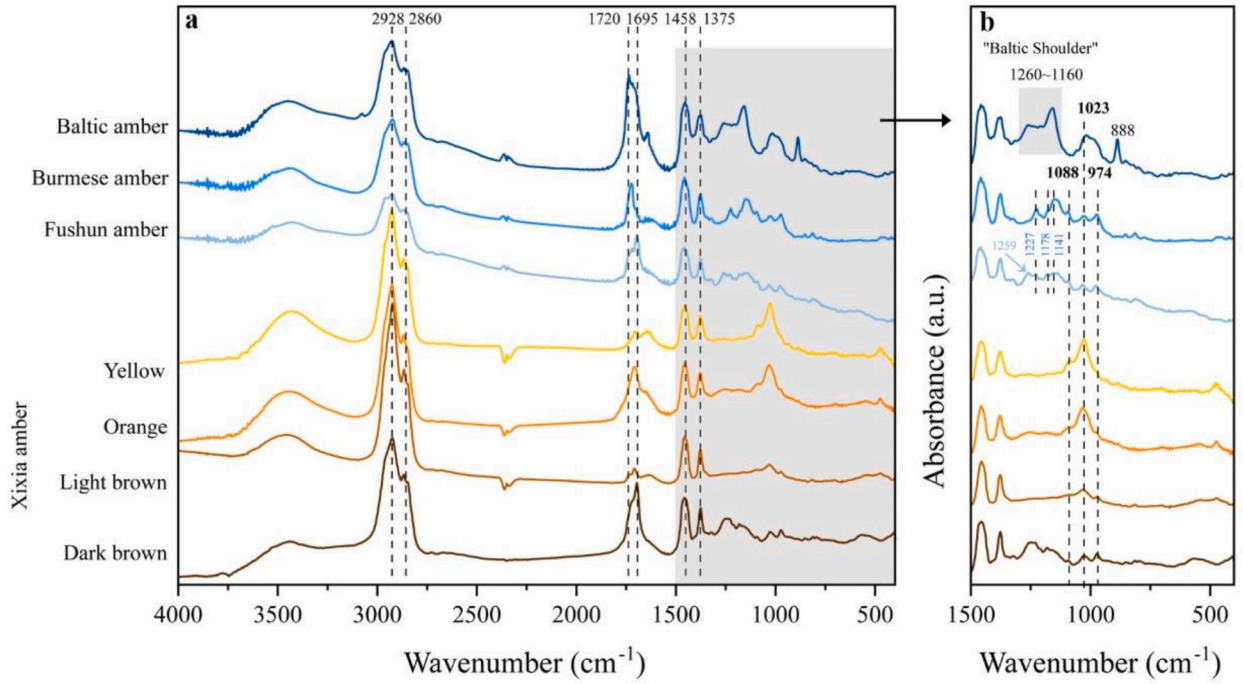

Fig. 6. FTIR spectra of ambers from the Baltic Sea, Burma, Fushun and Xixia: (a) spectra in the region of 4000~400 cm^{-1};(b) spectra in the region of 1500~400 cm^{-1}.

temperature of 480 °C for 10 s. The pyrolyzed samples were then transferred to the GC/MS system for gas chromatographic analysis. The GC was operated in split mode (50:1) and was equipped with an HP-5MS fusecsilica capillary column (5 % Phenyl Methyl Siloxane, 30 m × 0.25 mm i.d. × 0.25 μm film thickness). The GC oven operation conditions were: initial temperature held at 40 °C for 1 min, increased from 40 to 320 °C at a rate of 10 ′c min (held for 0.5 min). Helium was used in the constant flow mode at 1.0 mL/min. The mass spectrometer was operated in the electro impact mode at ionization energy of 70 eV and a source temperature of 230 °C. Full scan mass spectra were recorded over a mass range from 10 to 800 amu and data were acquired and processed using Chemstation software.

4. Results and discussions

4.1. Gemological properties of Xixia Amber

The specific gravity (SG) of the eight Xixia amber samples was found to span from 1.00 to 1.14, which is consistent with the typical range for amber SG values. The refractive indices (RI) of these samples, determined by employing the spot method, varied between 1.52 and 1.59, corroborating the established RI for amber. Each sample underwent UV illumination in a darkened environment using a 365 nm UV lamp, and their resulting fluorescent responses were recorded. These characteristics, summarized in Table 1, confirm the specimens' identification as amber, validated through standard gemological assessment procedures.

The rock specimen harboring the yellow amber (Fig. 4a) was meticulously collected and subsequently prepared as thin sections (Fig. 4b). Upon examination under polarized light microscopy, the presence of quartz, feldspar, and chlorite grains was revealed within the thin sections, these mineral constituents being held together by a matrix of argillaceous cement. The amber, rendered entirely opaque in images captured with crossed polarizers (Fig. 4d), is observed to be either clustered or irregularly interspersed amidst the aforementioned grains, thereby affirming its homogenous composition (Fig. 4c).

The Xixia amber samples primarily exhibited internal air bubbles of various sizes (5–50 μm), a common feature indicating their origin as tree resin. As shown in Fig. 5a-f, these bubbles are present across different colored samples, including yellow (Fig. 5a), light-brown (Fig. 5b), orange (Fig. 5c and d), and brown (Fig. 5e and f). Despite the color variations, the internal features remained consistent, predominantly consisting of air bubbles with no plant or insect tissues detected within the samples.

4.2. Infrared spectroscopy

The FTIR spectra depicted in the lower three curves of Fig. 6a for Xixia amber samples exhibit prominent peaks at wavenumbers 2928, 2860, 1709, 1458, 1375, 1025, and 974 cm^{-1}. These spectra were then compared with those of amber from two main important sources (Baltic and Burma) and a significant domestic Chinese source (Fushun), as illustrated in the upper three curves. The findings corroborate well with the previously documented FTIR spectra of Baltic amber [18–20], Burmese amber [11,21], and Chinese Fushun

Table 2
Positions and assignment of infrared absorption peaks of the amber [23,24].

Band (cm^{-1})	Functional groups
3080~3050	ν (CH)C=CH_2 group
3000~2800	ν (C–H) in aliphatic group
1740~1710	ν (C=O) in esters
1710~1690	ν (C=O) in acids
1643	ν (C=C conjugated)
1470~1440	δ (CH_2– CH_3)
1390~1360	δ (CH_2), δ (CH_3)
1250~1030	ν (C–O)
1023	ν (C–OH) in 1° and 2° alcohols (often doublet like signal (1023 and 974 cm^{-1}) [25]
888	vinylidene γ(R_2C=CH_2)

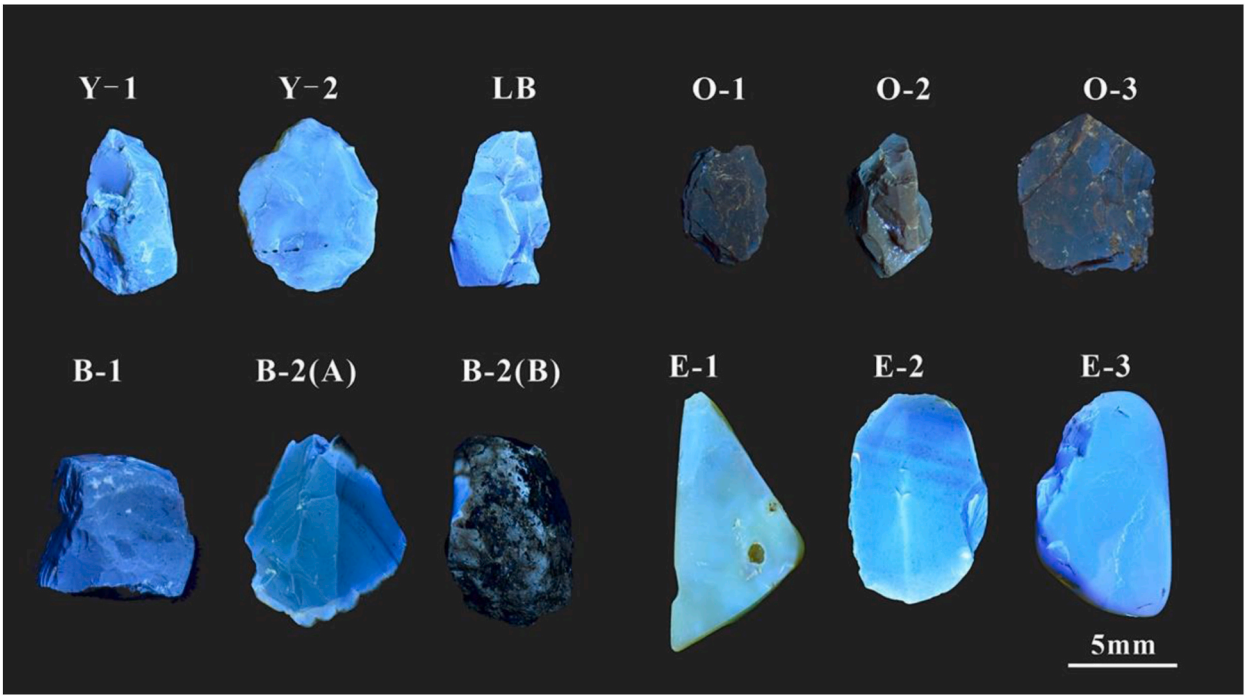

Fig. 7. Fluorescence phenomenon of amber samples under long-wave ultraviolet (UV) light.

amber [22]. Table 2 presents the assignment of the infrared spectral wavenumbers to their corresponding vibrational modes.

In the FTIR spectra of all Xixia amber samples from Henan, pronounced aliphatic absorptions were evident at wavenumbers 2930, 1454, and 1377 cm^{-1}, suggesting an aliphatic structure as the primary framework of the amber. The peak around 1709 cm^{-1} is characteristic of carbonyl groups [25]. A succession of moderate to weak absorption bands within the spectral region from 1260 to 1020 cm^{-1} implies the presence of oxygen-bearing functional groups, such as esters, alcohols, and ethers. The absence of peaks at 3048, 1642, and 888 cm^{-1} serves to verify the authenticity of the amber, distinguishing it from copal [26].

The band at 1740~1690 cm^{-1}, attributed to the carbonyl stretching vibration, is notably weaker in the yellow and light brown Xixia amber samples compared to those from other three origins. Conversely, this band exhibits a significantly increase within the orange and dark brown Xixia amber samples. It has been established that C=O group acts as a strong chromophore, and the color of amber tends to darken upon oxidation due to an elevated concentration of C=O groups [27], typically indicating a positive correlation. However, the observed color intensity in Xixia amber samples does not appear to correlate positively with the C=O concentration. Furthermore, the spectral band displays a high-frequency left shift and low-frequency right shift in the yellow and orange Xixia ambers, whereas it manifests a low-frequency left shift and high-frequency right shift in the light and dark brown Xixia ambers. This phenomenon could be indicative of varying relative concentrations of carboxylic acids and esters [7].

Furthermore, an examination of the infrared fingerprint region from 1350 to 400 cm^{-1} (Fig. 6b) enables the categorization of the samples into two distinct groups. The first group, comprising the yellow and orange samples, is characterized by a dominant peak at 1023 cm^{-1}. This peak often emerges as a bimodal feature alongside the 974 cm^{-1} peak, which is typically associated with the C–OH stretching vibrations in primary and secondary alcohols [25]. The second group consists of light and dark brown samples and the 1023 cm^{-1} and 974 cm^{-1} intensities of this group are comparable. In addition, the dark brown samples showed peaks 1259 cm^{-1}, 1227

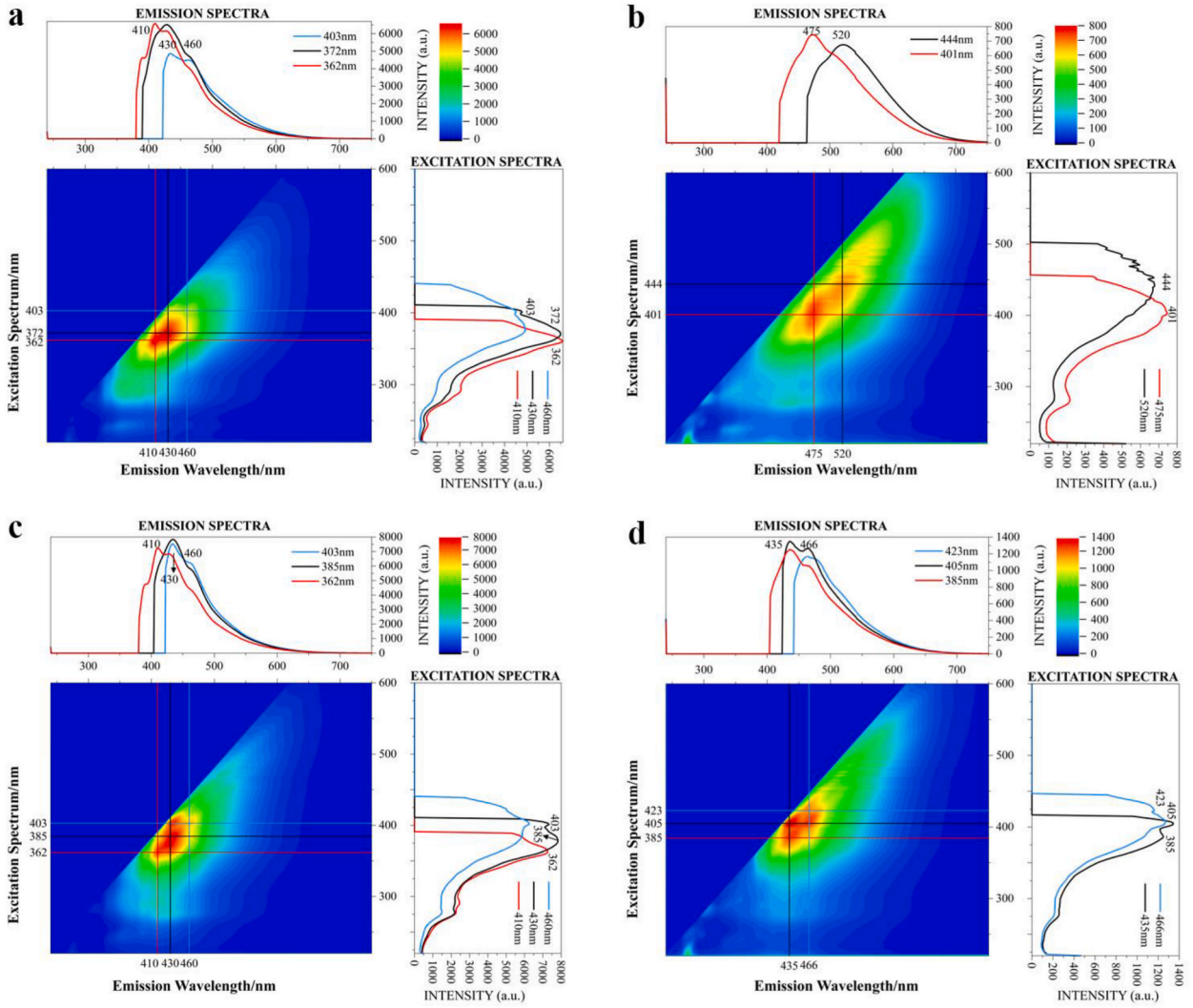

Fig. 8. 3D fluorescence spectra of Y-1(a), O-2 (b), LB(c) and B-1(d).

cm^{-1}, 1178 cm^{-1}, 1088 cm^{-1}, which were very similar to Fushun amber (1259 cm^{-1}, 1227 cm^{-1}, 1178 cm^{-1}, 1141 cm^{-1}, 1088 cm^{-1}), and the two could only be distinguished by the 1141 cm^{-1} peak in the infrared spectrum. This series of spectral peaks is related to the C–O stretching vibration of oxygen-containing functional groups [28].

Infrared spectroscopy analysis focusing on the morphology of the carbonyl bands and the characteristic doublet-like signal (1023 cm^{-1} and 974 cm^{-1}) suggests the presence of two unique types of Xixia amber.

The Xixia amber samples exhibit two primary varieties based on their oxidation-induced color changes and distinctive infrared spectral patterns.

1. **Lighter Variety (yellow to orange upon oxidation):** This variety is initially pale in color, presenting as yellow in newly extracted samples, and subsequently transitions to an orange hue as oxidation occurs. In the infrared spectra, this type is marked by carbonyl bands that display a pronounced intensity on the lower wavenumber side (left) and reduced intensity on the higher wavenumber side (right). Additionally, within the pair of peaks constituting the doublet-like signal, the peak at 1023 cm^{-1} is notably more prominent than the one at 974 cm^{-1}.
2. **Darker Variety (light to dark brown upon oxidation):** On the contrary, the darker variety of Xixia amber is identified by an initial light brown color in pristine samples, which progressively darkens to a deep brown upon exposure to oxidation. The characteristic carbonyl band in this variety exhibits lower intensity on the lower wavenumber side and increased intensity on the higher wavenumber side, with the doublet-like signal showing comparable intensities for both its constituent peaks.

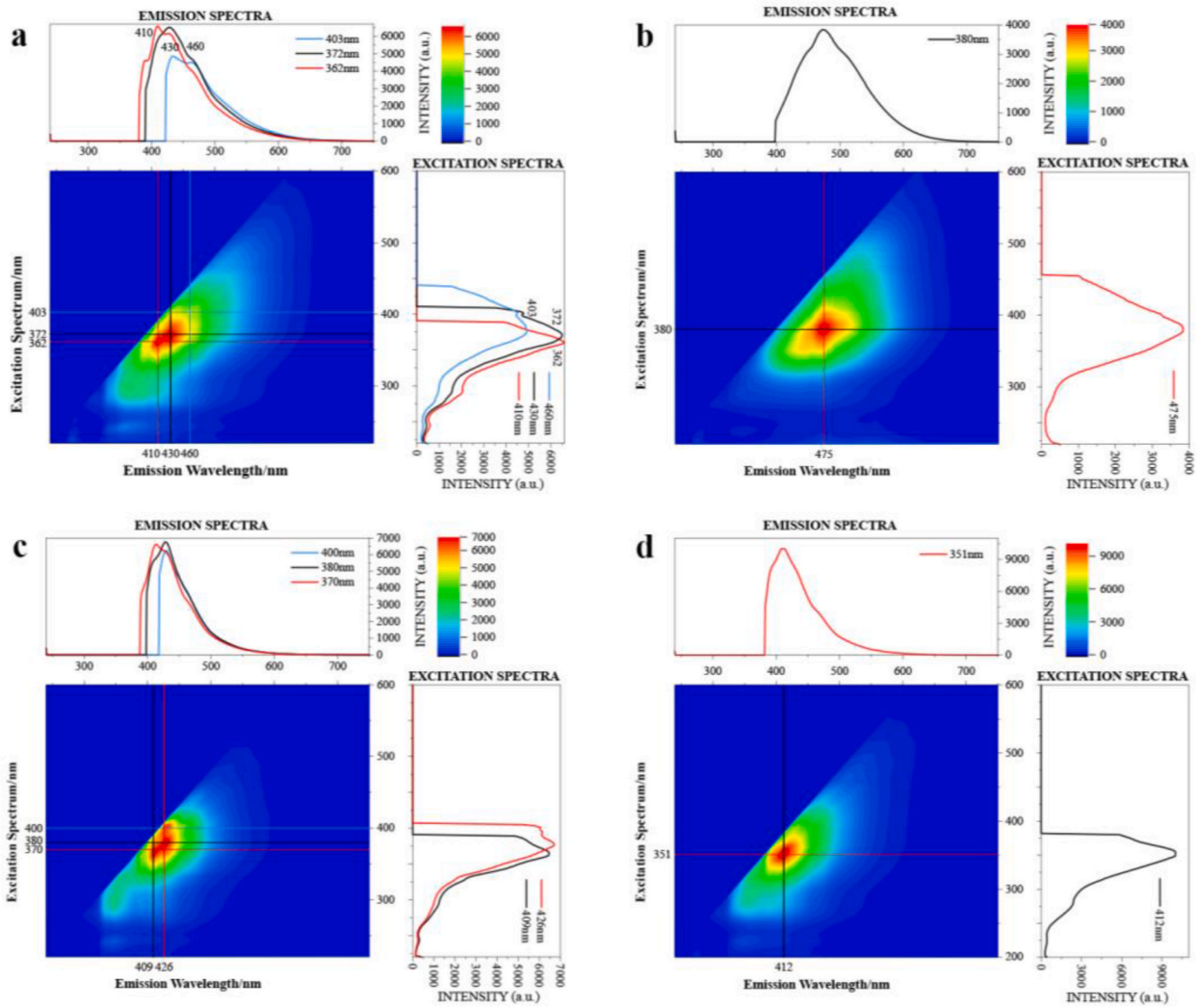

Fig. 9. 3D fluorescence spectra of Xixia yellow amber Y-1(a), Baltic yellow amber E−1(b), Burmese yellow amber E−2 (c) and Fushun yellow amber E−3(d).

4.3. Fluorescence

4.3.1. Long-wave UV radiation

The fluorescence phenomena of all independent samples under long wave ultraviolet radiation in this study are shown in Fig. 7, nearly all Xixia amber samples exhibit a faint to intense blue fluorescence. The fluorescence intensity, as observed by the naked eye, can be ranked as follows: yellow ≈ light brown > dark brown > orange. Compared to the reference samples, only the yellow and light brown Xixia amber have fluorescence intensities similar to theirs.

In general, the deepening color of amber correlates with increased oxidation, which in turn diminishes its fluorescence intensity accordingly. The presence of C=O (carbonyl) groups not only serves as a strong chromophore, but also functions to quench fluorescence due to the n→π* transition that occurs when C=O is linked to atoms with unpaired electrons. This transition has a very low molar absorption coefficient (approximately 10^2 L mol^{-1} cm^{-1}), potentially causing the amber's fluorescence to wane or even extinguish, while the fluorescent wavelength experiences a shift towards longer wavelengths [8]. As the C=O content increases, the ultraviolet fluorescence of amber gradually transitions from strong to weak, ultimately vanishing.

The dark-hued samples examined in this study (light brown and dark brown) exhibit a more intense body color compared to their orange counterparts, but their fluorescence intensity is stronger. This discrepancy may be attributed to factors other than oxidation, such as differences in elemental composition [29].

4.3.2. Three-dimensional fluorescence spectra

The 3D fluorescence spectra of Xixia amber samples (Fig. 8) were analyzed under uniform testing conditions. The spectra of samples

Table 3
Typical fluorescence peaks and corresponding best excitation light sources of yellow amber samples from different origins.

Origin	Typical fluorescence peaks (nm)	Corresponding best excitation light sources (nm)
Xixia, Henan	430	372
	410	362
The Baltic Sea	475	350
Burma	426	380
	409	370
Fushun, Liaoning	412	352

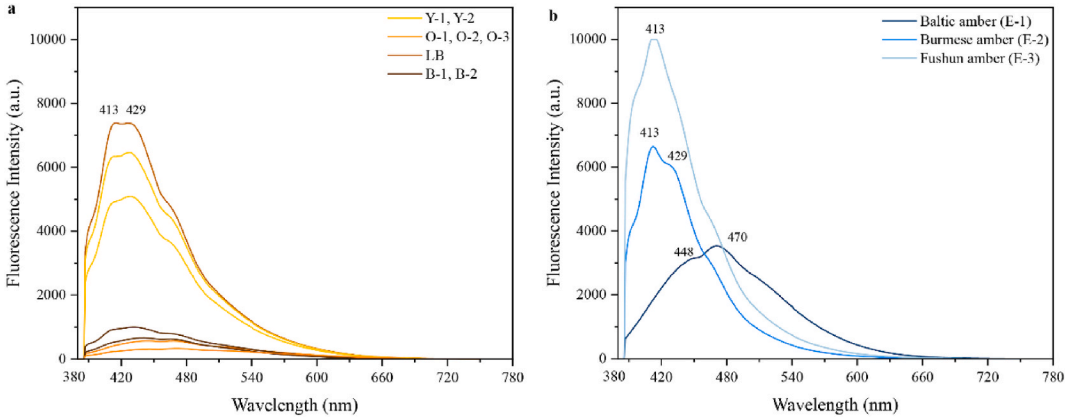

Fig. 10. Emission spectra of Xixia ambers (a) and reference samples (b) under 375 nm excitation wavelength.

with the same color have the same peak positions, so only one sample from each color group was selected for plotting. When comparing the relative fluorescence intensities based on the strongest fluorescence peak, the order from strongest to weakest is: light brown > yellow > dark brown > orange.

1. Yellow Sample (Fig. 8a): Excited with 372 nm light, the yellow sample's strongest fluorescence peak is at 430 nm in the violet region. Secondary emission centers are noted at 362 nm/410 nm, with a weaker one at 403 nm/460 nm. The relative fluorescence intensities for the strongest peak in these yellow samples exceed 5000.
2. Orange Sample (Fig. 8b): This sample shows a redshift in its emission, with the strongest fluorescence peak at E_X/E_M 401 nm/475 nm, and exhibits the lowest relative fluorescence intensity among all samples, all below 1000. This indicates a significant degree of oxidation.
3. Light Brown Sample (Fig. 8c): Exhibiting its most intense emission peak at 430 nm in the violet region, optimally excited at 385 nm, the light brown sample's strongest peak exceeds a relative fluorescence intensity of 7000. Additional fluorescence peaks at 362 nm/410 nm and 403 nm/460 nm shows similar intensities.
4. Dark Brown Sample (Fig. 8d): The strongest fluorescence peak for this sample occurs at EX/EM 405 nm/435 nm, with a relative intensity below 2000. A secondary peak is observed at EX/EM 405 nm/466 nm. Compared to the light brown sample, the dark brown sample demonstrates a redshift in emission peak position and a decrease in relative intensity, suggesting a higher oxidation level.

In general, as amber oxidizes, the characteristic peaks and emission centers of its fluorescence spectrum gradually shift towards longer wavelengths (redshift) and weaken in intensity. The orange sample, exhibiting the most significant redshift and lowest intensity, is identified as the most highly oxidized among the samples.

Fig. 9 illustrates the 3D fluorescence spectra of yellow amber from Xixia and reference sources. The spectral characteristics of the yellow Xixia sample have been described above, and the spectral characteristics of each reference type are as follows.

1. Baltic Amber (Fig. 9b): Exhibits a broad emission peak range from 380 to 600 nm. Under excitation by a 350 nm light source, its strongest fluorescence peak is around 475 nm, making it distinctive with the largest luminescence range and the longest wavelength among the strongest emission peaks.
2. Burmese Amber (Fig. 9c): The most intense fluorescence peak is centered at 426 nm, optimally excited at 380 nm, and can also be activated by light sources around 400 nm. Additionally, it displays another emission peak at 409 nm, with an optimal excitation wavelength of 370 nm.
3. Fushun Amber (Fig. 9d): Features its most prominent emission peak at 412 nm, best excited by a 352 nm light source.

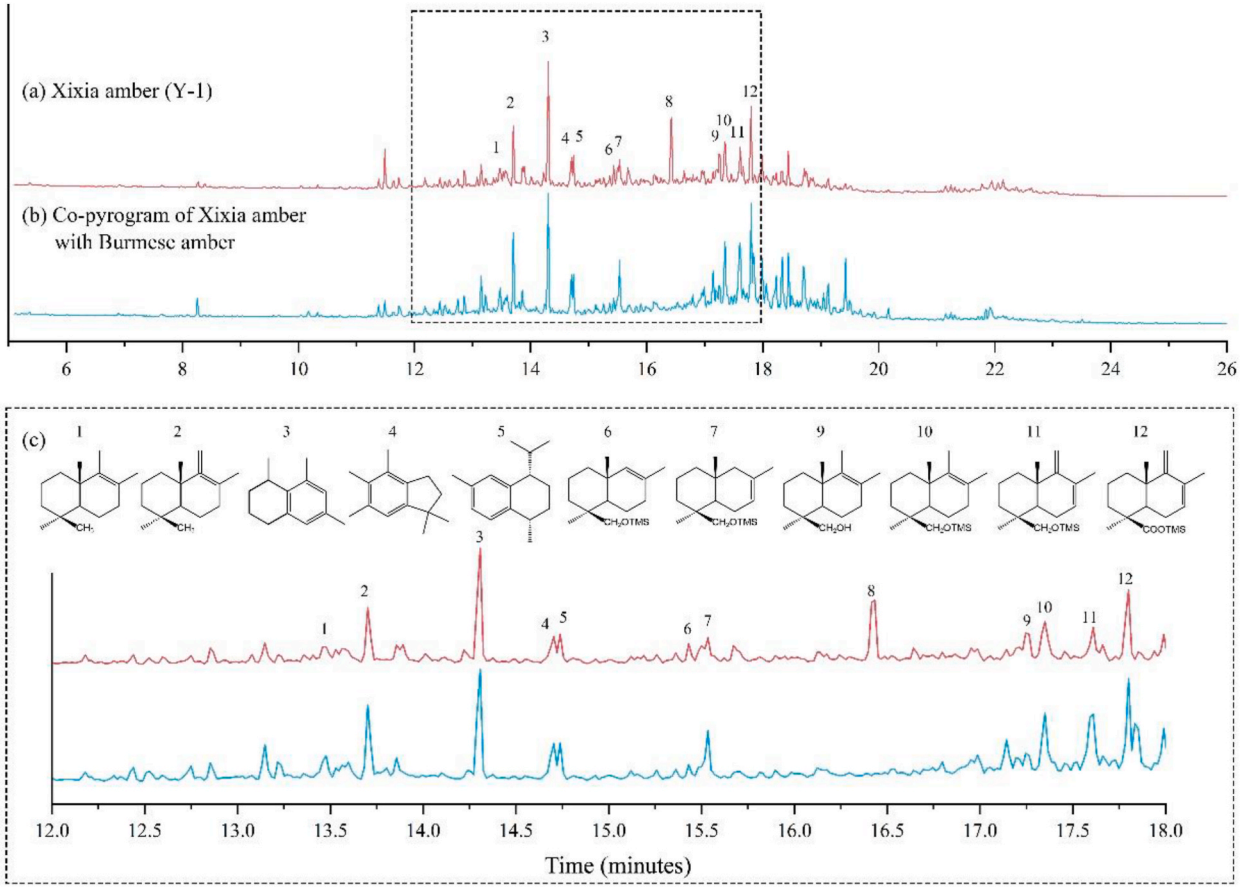

Fig. 11. Total ions chromatograms of Xixia amber (a) and Co-pyrogram of Xixia amber with Burmese amber(b). Framed areas (12–18 min) show partial pyrolyzates of esterified communol and communic acid. Labeled peaks and the corresponding chemical structures are also listed.

Table 3 presents the typical fluorescence peaks and their corresponding optimal excitation light sources for amber samples from different origins. A careful comparison of the three-dimensional fluorescence spectra reveals distinctive patterns.

- Baltic amber is the most distinguishable due to its extensive luminescence range and the prominent emission peak at 475 nm.
- The luminescence behavior of amber from Burma, Fushun, and Xixia is somewhat similar but can be distinguished by comparing the wavelengths of the strongest fluorescence peaks (Xixia > Burma > Fushun).
- The similarity in luminescent behavior between Burmese and Xixia amber is particularly due to comparable geological ages (Late Cretaceous) and botanical origins (*Araucariaceae* family) [17].

4.3.3. Two-dimensional fluorescence spectroscopy

The fluorescence characteristics of organic substances are comprehensively influenced by many factors, especially the excitation light source. The handheld longwave ultraviolet light source used during the shooting was centered at 365 nm. In order to further explain the fluorescence phenomenon under handheld longwave ultraviolet lamps, it is usually possible to compare the emission spectra of amber samples from different origins under 365 nm wavelength excitation in their three-dimensional fluorescence spectra [30]. The emission spectra of the sample were collected under excitation at a wavelength of 365 nm, and the two-dimensional fluorescence spectra plotted are shown in Fig. 10.

As depicted in Fig. 10a, the Xixia amber samples exhibit strong emission peaks at 413 nm and 429 nm, resulting in a blue fluorescence with a purple tone under handheld long-wave UV lamp illumination. This fluorescence intensity diminishes with increasing oxidation, aligning with observations made by the naked eye (Fig. 7). In comparison, the reference samples of Baltic, Burmese, and Fushun amber (Fig. 10b) display varying emission characteristics. Baltic amber shows a broader luminescence range with a prominent peak at 470 nm, resulting in a distinct green light fluorescence, making it easily distinguishable from the others. Conversely, Burmese and Fushun ambers have their strongest emission peaks in the blue-purple region around 424 nm, indicating similar fluorescence properties compared to Xixia amber.

Table 4
List of compounds corresponding to marked peaks in Fig. 11.

Peak no.	Compound	Base peak	Molecular ion
1	Biformene pyrolyzate IIId	191	206
2	Biformene pyrolyzate IVd	191	222
3	Naphthalene, 1,2,3,4-tetrahydro-1,6,8-trimethyl-*	159	174
4	1,1,4,5,6-Pentamethyl-2,3-dihydro-1H-indene*	173	188
5	Naphthalene, 1,2,3,4-tetrahydro-1,6-dimethyl-4-(1-methylethyl)-, (1S-cis)- *	159	202
6	Communol pyrolyzate Ic	73	280
7	Communol pyrolyzate IIc	107	280
8	Unassigned	163	206
9	Communol pyrolyzate IIIb	95	222
10	Communol pyrolyzate IIIc	73	294
11	Communol pyrolyzate IVc	132	292
12	Communic acid pyrolyzate IVa	173	306

Mass spectral data correspond to the trimethylsilyl derivatives. Assignments were made based on the Agilent NIST 17 Mass Spectral Library (indicated with an asterisk, Match >900) and published reference data [34].

4.4. Py (HMDS)-GC-MS

To further elucidate the molecular-level similarities between Xixia amber and Burmese and Fushun amber, pyrolysis gas chromatography-mass spectrometry (py-GC-MS) was employed to differentiate the types of Xixia amber. The chemical classification of ambers is grounded in their molecular structure. Class I ambers originate from the resin of higher plants, primarily characterized by polymers of labdatriene diterpenes. Within the geosphere, ambers based on *regular* and *enantio* labdanoids are widely recognized. Sub-classification within Class I ambers is established on the distinction between these labdanoids and is further influenced by the presence or absence of succinic acid incorporation [31,32].

One crucial method for confirming the type of resinous fossil is the application of py-GC-MS. This technique utilizes the thermal decomposition products of labdanoid diterpenes to ascertain the classification of fossil resinite. The retention times of these substances in this study primarily concentrate in the 12–18 min range. The classification of Xixia amber types was determined by contrasting the test results of individual samples (Fig. 11a) with co-pyrogram of Burmese amber (Class Ib) (Fig. 11b). Compounds identification was achieved through comparison with the NIST library and existing studies [33,34].

In Fig. 11c, portions of the chromatograms have been enlarged (12–18 min) to emphasize a segment that encompasses a sequence of newly discovered compounds. Peaks within this region are labeled as 1–12 in the figure and are listed in Table 4. Except for compounds 3, 4, 5, and 8, the remaining substances in Fig. 11c represent partial pyrolysis products of esterified communic acid (Ia ~ IVa) and communol (Ib ~ IVb and Ic ~ IVc) moieties within the macromolecular structure in the presence of HMDS. These findings indicate that Xixia amber belongs to the regular configuration, additionally lacking succinic acid, confirming its classification as Class Ib. The same MS classification provides a more comprehensive explanation for the similarities between Xixia amber and Burmese and Fushun amber.

5. Conclusions

Xixia amber presents with a range of yellow-brown hues, varying degrees of translucency, fragility, and inclusions of internal bubbles. It can be differentiated into two primary types based on coloration, infrared spectral characteristics, and luminescence properties. Both types encompass examples that are relatively fresh as well as those that have undergone oxidation. The lighter series of colors transitions from a yellow appearance in fresh samples to an orange hue upon oxidation. Conversely, the darker series features light brown in its fresh state, darkening to dark brown as oxidation occurs.

The distinction between the two series is clearly defined in the infrared spectra by the unique morphology of the carbonyl bands and the presence of a doublet-like signal at 1023 cm^{-1} and 974 cm^{-1}. When examining luminescence behavior, the darker series exhibits a more intense fluorescence compared to the lighter series for both fresh and oxidized samples. In the 3D fluorescence spectrum, the most potent emission wavelength (430 nm) remains consistent across both series. However, the optimal excitation wavelength varies, being 372 nm for the yellow samples and 385 nm for the light brown samples.

The majority of Xixia amber samples belong to the light color series. To better understand their characteristics, we compared the yellow samples with yellow ambers from other origins, specifically the Baltic Sea, Burma, and Fushun, China. The results indicate that Xixia amber, though exhibiting similar gemological traits to other ambers, displays distinctive infrared spectral features, especially in the fingerprint region. Xixia amber's fluorescence behavior aligns more closely with Burmese and Fushun amber rather than Baltic amber, with distinctions in the peak wavelengths of the strongest fluorescence, following the order: Xixia > Burmese > Fushun. The py-GC-MS results indicate that Xixia Amber belongs to Class Ib, explaining, to some extent, the similarities among these three, characterized by a regular configuration and the absence of succinic acid.

CRediT authorship contribution statement

Yan Li: Writing – review & editing, Project administration, Funding acquisition. **Yilei Feng:** Writing – original draft, Methodology,

Investigation, Formal analysis. **Jingfen Du:** Resources. **Yamei Wang:** Data curation. **Guanghai Shi:** Resources. **Youzhi Liang:** Resources.

Declaration of competing interest

The authors declare the following financial interests/personal relationships which may be considered as potential competing interests: Yan LI reports financial support was provided by China University of Geosciences. No If there are other authors, they declare that they have no known competing financial interests or personal relationships that could have appeared to influence the work reported in this paper.

Acknowledgements

The work has been supported by Hubei Gem & Jewelry Engineering Technology Center (No. CIGTXM-03-202304) and Hubei Philosophy and Social Science Program Project (No.21G007). The project was also supported by the "CUG Scholar" Scientific Research Funds at China University of Geosciences (No.2022185).

References

[1] A. Ross, Amber, Harvard University Press, 1998.
[2] Y. Wang, Amber Gemology, China University of Geosciences Press, Wuhan, 2019.
[3] Y. Li, D. Zheng, J. Sha, H. Zhang, S. Denyszyn, S.-C. Chang, *Lower cretaceous hailar amber: the oldest-known Amber from China*, cretac, Res. 145 (2023) 105472.
[4] S. Zhou, S. Zhao, Initial study on the xixia-neixiang amber deposit of henan, Miner. Resour. Geol. 19 (2005) 57.
[5] X. Xu, Ancient Chinese amber arts: shang to yuan, Palace Mus. J. 112 (2009).
[6] T. Zhao, M. Peng, M. Yang, R. Lu, Y. Wang, Y. Li, Effects of weathering on FTIR spectra and origin traceability of archaeological amber: the case of the han tomb of haihun marquis, China, J. Archaeol. Sci. 153 (2023) 105753.
[7] G. Pastorelli, Y. Shashoua, J. Richter, Hydrolysis of baltic amber during thermal ageing - an infrared spectroscopic approach, Spectroc. Acta Pt. A-Molec. Biomolec. Spectr. 106 (2013) 124.
[8] X. Li, Y. Wang, G. Shi, R. Lu, Y. Li, Evaluation of natural ageing responses on Burmese amber durability by FTIR spectroscopy with PLSR and ANN models, Spectroc. Acta Pt. A-Molec. Biomolec. Spectr. 285 (2023) 121936.
[9] J. Park, E. Yun, H. Kang, J. Ahn, G. Kim, *IR and py/GC/MS Examination of amber relics Excavated from 6th century royal Tomb in Korean peninsula*, spectroc. Acta Pt. A-molec, Biomolecules 165 (2016) 114.
[10] Y. Bai, X. Zheng, Z. Yin, Characterization of Burmese amber with three-dimensional fluorescence, Spectrosc. Spectr. Anal. 40 (2020) 1473.
[11] X. Jiang, Z. Zhang, Y. Wang, F. Kong, Gemmological and spectroscopic characteristics of different varieties of amber from the hukawng valley, Myanmar, J. Gemmol. 37 (2020) 144.
[12] G. Zhang, Evolution of the late cretaceous depositional systems in the Xixia bsain, henan Province, Jiaozuo Inst. Technol. (Nat. Sci.) 85 (2002).
[13] S. Guo, X. Yan, Y. Sun, Y. Hong, Analysis of Chinese amber, J. Fudan Univ. Nat. Sci. 271 (1991).
[14] G. Li, P. Chen, D. Wang, D.J. Batten, *The spinicaudatan Tylestheria and biostratigraphic Significance for the Age of dinosaur Eggs in the upper cretaceous Majiacun formation, Xixia Basin, henan Province, China*, cret, Res. 30 (2009) 477.
[15] D. Wang, P. Chen, J. Chen, M. Cao, H. Pan, Discovery of invertebrate fossils from the dinosaurian egg-bearing strata in the Xixia Basin of henan, China, Acta Palaeontol. Sin. 483 (2006).
[16] G. Cao, L. Gao, Y. Lin, Y. Wang, X. Zu, *Discovery and Significance of the palaeoseismic Events in the late cretaceous Xixia and xiaguan basin*, sedim, Geol. Tethyan Geol. 30 (2010) 11.
[17] G. Shi, S. Dutta, S. Paul, B. Wang, F.M.B. Jacques, Terpenoid compositions and botanical origins of late cretaceous and Miocene amber from China, PLoS One 9 (2014) e111303.
[18] C. Beck, E. Wilbur, S. Meret, D. Kossove, K. Kermani, The infrared spectra of amber and the identification of baltic amber, Archaeometry 8 (1965) 96.
[19] M. Guiliano, L. Asia, G. Onoratini, G. Mille, Applications of diamond crystal ATR FTIR spectroscopy to the characterization of ambers, Spectroc. Acta Pt. A-Molec. Biomolec. Spectr. 67 (2007) 1407.
[20] A.P. Wolfe, R. Tappert, K. Muehlenbachs, M. Boudreau, R.C. McKellar, J.F. Basinger, A. Garrett, A new proposal concerning the botanical origin of baltic amber, Proc. Biol. Sci. 276 (2009) 3403.
[21] Z. Shi, C. Xin, Y. Wang, Spectral characteristics of unique species of Burmese amber, Minerals 13 (2023) 151.
[22] B. Wang, et al., A diverse paleobiota in early eocene Fushun amber from China, Curr. Biol. 24 (2014) 1606.
[23] O.R. Montoro, J. Tortajada, Á. Lobato, V.G. Baonza, M. Taravillo, Theoretical (DFT) and experimental (Raman and FTIR) spectroscopic study on communic acids, main components of fossil resins, Spectroc. Acta Pt. A-Molec. Biomolec. Spectr. 224 (2020) 117405.
[24] R.H. Brody, H.G.M. Edwards, A.M. Pollard, A study of amber and copal samples using FT-Raman spectroscopy, Spectroc. Acta Pt. A-Molec. Biomolec. Spectr. 57 (2001) 1325.
[25] E. Wagner-Wysiecka, Mid-infrared spectroscopy for characterization of baltic amber (succinite), Spectroc. Acta Pt. A-Molec. Biomolec. Spectr. 196 (2018) 418.
[26] X. Delclòs, E. Peñalver, V. Ranaivosoa, M.M. Solórzano-Kraemer, Unravelling the mystery of "Madagascar copal": age, origin and preservation of a recent resin, PLoS One 15 (2020) e0232623.
[27] Y. Wang, M. Yang, S. Nie, F. Liu, Gemmological and spectroscopic features of untreated vs. Heated amber, J. Gemmol. 35 (2017) 530.
[28] Y. Wang, G. Shi, W. Shi, R. Wu, Infrared spectral characteristics of ambers from three main sources (baltic, Dominica and Myanmar), Spectrosc. Spectr. Anal. 35 (2015) 2164.
[29] Y. Wang, M. Yang, P. Niu, Ananlysis on organic elements and content variation of ambers, treated ambers and copals from different producing areas around the world, J. Gems Gemmol. 16 (2014) 10.
[30] Z. Zhang, X. Jiang, Y. Wang, A.H. Shen, F. Kong, Fluorescence spectral characteristic of amber from Baltic Sea region, Dominican republic, Mexico, Myanmar and China, J. Gems Gemmol. 22 (2020) 1.
[31] K.B. Anderson, R.E. Winans, R.E. Botto, The nature and fate of natural resins in the geosphere—II. Identification, classification and nomenclature of resinites, Org. Geochem. 18 (1992) 829.
[32] J. Poulin, K. Helwig, Class id resinite from Canada: a new sub-class containing succinic acid, Org. Geochem. 44 (2012) 37.
[33] K.B. Anderson, The nature and fate of natural resins in the geosphere Part XI.† ruthenium tetroxide oxidation of a mature Class Ib amber polymer‡, Geochem. Trans. 2 (2001) 1.
[34] J. Poulin, K. Helwig, Inside amber: new insights into the macromolecular structure of Class Ib resinite, Org. Geochem. 86 (2015) 94.